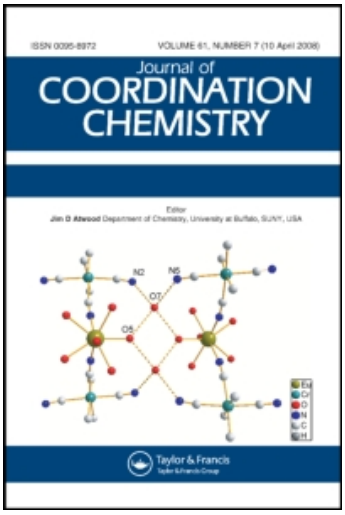

Journal of Coordination Chemistry
Publication details, including instructions for authors and subscription information:
http://www.informaworld.com/smpp/title~content=t713455674

Aluminium(III) complexes of *S*-histidine: synthesis, characterization and potentiometric and spectroscopic study of solution equilibria

Predrag Djurdjevic[a]; Mirjana Cvijovic[b]; Joanna Zakrzewska[c]
[a] Faculty of Science, Institute of Chemistry, 34000 Kragujevac, State Union of Serbia and Montenegro [b] The Copper Mill, Sevojno, 31000 Uzice, State Union of Serbia and Montenegro [c] Institute of General and Physical Chemistry, 11000 Belgrade, State Union of Serbia and Montenegro

To cite this Article Djurdjevic, Predrag , Cvijovic, Mirjana and Zakrzewska, Joanna(2005) 'Aluminium(III) complexes of *S*-histidine: synthesis, characterization and potentiometric and spectroscopic study of solution equilibria', Journal of Coordination Chemistry, 58: 17, 1615 — 1629
To link to this Article: DOI: 10.1080/00958970500258807
URL: http://dx.doi.org/10.1080/00958970500258807

Journal of Coordination Chemistry
Vol. 58, No. 17, November 2005, 1615–1629

Aluminium(III) complexes of *S*-histidine: synthesis, characterization and potentiometric and spectroscopic study of solution equilibria

PREDRAG DJURDJEVIC*†, MIRJANA CVIJOVIC‡ and JOANNA ZAKRZEWSKA§

†Faculty of Science, Institute of Chemistry, P.O. Box 60, 34000 Kragujevac, State Union of Serbia and Montenegro
‡The Copper Mill, Sevojno, 31000 Uzice, State Union of Serbia and Montenegro
§Institute of General and Physical Chemistry, 11000 Belgrade, State Union of Serbia and Montenegro

(*Received 28 February 2005; in final form 22 June 2005*)

Complex formation between *S*-histidine (HHis) and aluminium(III) ion in aqueous solution was studied by potentiometric measurements, ESI-MS, ^{27}Al and ^{13}C NMR spectroscopy at 298 K. Potentiometric titrations were made at 298 K over the pH range 1.90 to 6.40 on solutions with total aluminium concentrations from 1.0 to 20.0×10^{-3} mol dm^{-3}. Ionic strength of the solutions was maintained at 0.1 mol dm^{-3} with LiCl. A neutral solution of HHis was used as titrant. Non-linear least-squares treatment of the pH 3.0–6.2 data indicated the formation of one main complex, $Al_2(OH)His^{4+}$, and two minor ones, $Al(HHis)^{3+}$ and $Al(HHis)His^{2+}$, with overall formation constants, $\beta_{p,q,r}$ (p, q, r being stoichiometric coefficients for metal, ligand and proton, respectively), of $\log \beta_{2,1,-1} = 6.15 \pm 0.09$, $\log \beta_{1,1,1} = 12.15 \pm 0.10$, $\log \beta_{1,2,1} = 20.1 \pm 0.08$, respectively. The complex $Al(His)^{2+}$, with a stability constant $\log \beta_{1,1,0} = 7.21 \pm 0.08$ was at the limit of the detection and is probably the mixed hydroxo complex, $Al(OH)HHis^{2+}$. ESI-mass spectra generally confirmed the equilibrium model though a variety of polynuclear hydrolytic complexes was observed. ^{27}Al NMR spectra of solutions with aluminium concentrations of $5–50 \times 10^{-3}$ mol dm^{-3} and histidine concentrations of $25–260 \times 10^{-3}$ mol dm^{-3} were recorded. In the pH interval 4.0–4.5 a resonance at 4.7 ppm was assigned to $Al_2(OH)His^{4+}$, while at pH 5.0–6.1 two resonances at 8.2 and 12.0 ppm were assigned to $Al(HHis)^{2+}$ and $Al(HHis)(His)^{2+}$ [or $Al(OH)(HHis)_2^{2+}$], respectively. In ^{13}C NMR spectra the upfield chemical shift difference of the carboxyl carbon resonance of free and bound histidine of 0.8 ppm, and that of aliphatic α- and β-carbons of 0.3–0.4 ppm, confirmed the formation of the complex in which both the carboxyl and amino groups of histidine participate in coordination. An isolated complex has the composition $[(AlOH)(HHis)_2]Cl_2$. IR spectra showed changes in position and profile of carboxyl and amino bands as compared to those of free *S*-histidine, again indicating the involvement of both groups in coordination to aluminium.

Keywords: Aluminium; *S*-Histidine; Complex formation; Synthesis; Stability constants

*Corresponding author. Email: preki@knez.kg.ac.yu

Journal of Coordination Chemistry
ISSN 0095-8972 print: ISSN 1029-0389 online © 2005 Taylor & Francis
DOI: 10.1080/00958970500258807

1. Introduction

Aluminium can be a detrimental and toxic element. It may enter the human body from the environment, the diet or medication, and pass into systemic circulation from the gastrointestinal (gi) tract or lungs, or by the parenteral route (hemodialysis or parenteral nutrition) [1–3]. Because Al^{3+} is a hard metal ion, it forms complexes of highest stability with ligands containing hard donor groups. Most effective are ligands possessing strongly basic, negatively charged oxygen atoms (phenolates, alcoxides, carboxylates, phosphonates, etc.) and nitrogen atoms appropriately arranged to form five- or six-membered rings, such as aminocarboxylates [4–6]. Although amino acids generally do not form strong complexes with Al(III), those with appropriate side chains (glutamic, aspartic acids), can form chelates of appreciable stability on account of favourable steric arrangements of donor groups [7–11].

Among the amino acids, *S*-histidine is unique in that it has an imidazole group that may bind to a metal ion and is a component of proteins and enzyme active sites. The histidine possesses four potential coordination sites, the carboxyl group, the amino group, and the nitrogen atoms of the imidazole residue. The tertiary nitrogen is among the strongest electron donors and its Lewis basicity depends on the protonation state of the rest of the molecule and, in proteins, on the vicinity of carboxylate groups. It can thus serve as a site for aluminium complexation. Histidine mainly acts as a bidentate ligand via the amino–imidazolic couple or the amino–carboxylate couple. The third possible couple involving imidazole nitrogen–carboxylate is not favoured due to the formation of a seven-membered ring [12].

The solution chemistry of aluminium ion and histidine may be of importance in elucidating interactions between protein hydrolyzates used in parenteral nutrition and aluminium that is unavoidably present in such solutions. In addition, histidine taken as a food supplement may interact with concomitantly administered aluminium based antacids. Sites of aluminium–histidine interaction may involve the gi tract, blood, kidney tissue, cell cytosol and lysosomes. In the gi tract histidine is released from food and may reach appreciably high concentrations in the duodenum, jejunum and ileum and may interact with aluminium [13]. Histidine taken either for therapeutic purposes or released from ingested food may affect the solubilization of aluminum and enhance its bioavailability. In blood, levels of histidine may be quite appreciable in cases of total parenteral nutrition involving protein hydrolyzate, or in some diseases such as histidinemia, renal failure or Reye's syndrome [14]. Histidine can interact with the ultrafiltrable fraction of aluminium in serum, though such interactions are expected to be weak in comparison with those involving carboxylic acids or phosphate [7]. High levels of histidine may be expected in lysosomes and tissues rich in these cell organelles such as kidney tissue [15,16], especially in the case of ingestion of protein rich food. Taking all of the above into account, it is clear that an understanding of the nature of aluminium–*S*-histidine interactions would help in an understanding of aluminium toxicity.

The objective of the present work was to study complex formation between aluminium ion and *S*-histidine with respect to speciation, stability and binding mode. A review of available literature showed that no unambiguous description of aluminium complexation with *S*-histidine exists. Duc and coworkers [17] studied complexation of aluminium with the α-amino acids that constitute collagen by potentiometric measurements in $0.5\,\mathrm{mol\,dm^{-3}}$ $NaClO_4$ at 298 K. With histidine, a mononuclear,

mixed hydroxo complex was found. Dayde *et al.* [7] studied complexation of aluminium ion with glycine, serine, threonine and histidine in 0.15 mol dm^{-3} NaCl at 37°C by potentiometry and ^{1}H and ^{13}C NMR spectroscopy. The complex $Al_2(His)H_{-2}^{3+}$ was identified, with an overall stability constant $\log \beta_{2,1,-2} = 1.16 \pm 0.12$. In previous work [18], the complexes $Al(HHis)^{3+}$ ($\log \beta_{1,1,1} = 12.21 \pm 0.08$), $Al(His)^{2+}$ ($\log \beta_{1,1,0} = 7.25 \pm 0.08$) and $Al(HHis)(His)^{2+}$ ($\log \beta_{1,2,1} = 20.3 \pm 0.1$) were identified by potentiometric measurements in 0.1 mol dm^{-3} LiCl at 298 K. Here a study of complex formation involving potentiometry, ESI-MS, and ^{27}Al and ^{13}C NMR spectroscopy is reported. The main complex formed in aluminium–histidine solutions at a pH near 6, was synthesized and characterized.

2. Experimental

An aluminium chloride stock solution was prepared by dissolving $AlCl_3 \cdot 6H_2O$ in doubly distilled water. An appropriate amount of 0.1 mol dm^{-3} of HCl was added to prevent initial hydrolysis. Aluminium content was determined gravimetrically by precipitation with ammonia or 8-hydroxyquinoline. Both methods gave the same results within 0.3%. Concentration of free acid was determined potentiometrically with standard NaOH. *S*-Histidine was dissolved in doubly distilled water and assayed potentiometrically. The sodium hydroxide solution was prepared from a concentrated volumetric solution by diluting with freshly-boiled, doubly distilled water and cooling under a constant flow of purified nitrogen. Alkali concentration was checked by titration against potassium hydrogen phthalate. Hydrochloric acid solutions were standardized against tris(hydroxymethyl)aminomethane.

2.1. *Instruments and procedures*

All pH measurements were made using Beckman 4500 digital pH/mV meter (resolution ± 0.002 pH units or ± 0.1 mV) equipped with a Beckman combined electrode. Potentiometric titrations were performed in a thermostatted vessel at 298.0 ± 0.1 K and at constant ionic strength (0.1 mol dm^{-3} LiCl) under dinitrogen. The acidified aluminium solution was titrated with a neutralized solution of histidine [19]. Before commencing titrations, aluminum solutions were allowed to stand for 24 h. The titrant was added in small aliquots (0.005–0.01 cm^3) using a Metrohm Dosimat model 665, under energetic stirring of the solution. Potential (or pH) readings were taken every 2 min until a steady value of ± 0.1 V (±0.002 pH) was obtained. Usually, stable potentials were obtained after 5–10 min at the beginning of the titration (pH < 3) and after 20–25 min at pH > 3. All titrations were carried out in duplicate with agreement between replicates of around 5%. The electrode was calibrated to hydrogen ion concentration using a previously described method [7] before each experiment; determined pK_w was 13.65 ± 0.02. Species were characterized by the general equilibrium

$$pAl + qHis + rH = Al_p(His)_qH_r$$

and corresponding stability constants are given by

$$\beta_{p,q,r} = \frac{[\mathrm{Al}_p(\mathrm{His})_q\mathrm{H}_r]}{[\mathrm{Al}]^p[\mathrm{His}]^q[\mathrm{H}]^r}$$

where His is non-protonated ligand. Fully protonated histidine is denoted as H_3His^{2+}. Concentration stability constants of complexes, $\beta_{p,q,r}$, were calculated with the aid of the computer programs Hyperquad [20] and Superquad [21]. Complex formation constants were determined using four independent titrations with aluminium ion concentrations ranging from 1.0 to 20.0 mmol dm^{-3}; pH-metric data between 3.0 and 6.2 were used.

Complexation with amino acids competes rather weakly with aluminium hydrolysis and is thus difficult to investigate. To derive a reliable complexation model very accurate data for hydrolysis of aluminum are needed. Pronounced hydrolysis of aluminium ion could obscure weak complexation in solution [1]. Furthermore, polynuclear hydrolytic species, whose rate of formation is quite slow, may persist metastably for long periods and supersaturation with respect to hydrated aluminium oxides could further complicate the titration. To make sure that measured pH effects are due to complexation, relatively high concentration ratios of ligand to aluminium should be used and several experimental techniques combined. The diversity of factors that influence the hydrolysis is such that there is a number of models for aluminium hydrolysis. In the millimolar range of total aluminium concentrations over the pH interval from *ca* 3 to 5 the common consensus is that $Al(OH)^{2+}$, an oligomer, and $[Al_{13}O_4(OH)_{24}(H_2O)_{12}]^{7+}$ (Al_{13}-mer) are the main solution species [22]. However, based on previous work using 0.1 mol dm^{-3} LiCl at 298 K [18] and previously reported models [1,6], for the analysis of the titration curves the hydroxo species AlH_{-1} ($\log\beta = -5.27$), Al_3H_{-4} (−13.81), AlH_{-4} (−23.1), $Al_{13}H_{-32}$ (−106.5) and AlH_{-3}(aq) (−14.68) were taken into account.

ESI-MS was performed using an Agilent LC/MSD system. Aluminum–histidine solutions were prepared in the histidine to aluminum concentration range 1 : 1 to 5 : 1 at pH 4.20 and a total aluminum concentration of 50.0 mmol dm^{-3}. Solutions were allowed to stand for 5 days before final adjustment of pH. All data were acquired in the positive ion mode and processed using HP ChemStation software. IR spectra (KBr pellets) were recorded using a Perkin–Elmer 983G spectrophotometer. ^{27}Al NMR spectra were recorded at 104.26 and 130.28 MHz on Bruker MSL 400 and DRX 500 spectrometers, respectively, with $AlCl_3$ in 6 mol dm^{-3} HCl as external standard; D_2O was added as a lock. Measurement conditions were pulse width 7 μs, flip angle 45°, acquisition time, 98.3 ms, spectral width 20,833 Hz, number of transients 200–500, pulse repetition time, 1 s, number of data points 4k, digital resolution 10.17 Hz/point or 1.27 Hz/point (DRX500). A Bruker MSL 400 spectrometer was used for recording ^{13}C NMR spectra at 100.614 MHz. Some 16,000–18,000 transients were accumulated with a digital resolution 2.65 Hz per point. Samples were dissolved in D_2O and chemical shifts are referenced to dioxane as an external standard. Thermal analysis was performed using a Perkin–Elmer DSC 7 analyzer and Perkin–Elmer TGS2 thermogravimetric balance.

2.2. *Synthesis*

The Al^{3+}-*S*-histidine was obtained from the reaction of 50 mmol of aluminium chloride and 150 mmol of *S*-histidine in water. The pH of the mixture was adjusted to 5.90 with 1 mol dm^{-3} NaOH to give a total volume of 10 cm^3. The solution was gently stirred at 42°C for 1 day, cooled to room temperature and stirred under vacuum until the volume was considerably reduced. Further lowering of temperature induced the precipitation of unreacted histidine. The remaining filtered solution was further evaporated under vacuum and then cooled. The precipitate that formed was washed with ice-cold water, ethanol and ether and dried in air. Al content was analysed by ARL 3580B ICP/OES and DC-ARC plasma spectrometers [23]; chloride content was determined volumetrically. Anal. Calcd for $[Al(HHis)(His)]Cl_2$ (%): Al, 6.60; Cl, 17.2; C, 35.3; N, 20.6; H, 4.65. Found: Al, 6.8 (ICP), 6.7 (ARC); Cl, 17.7; C, 35.9; N, 21.0; H, 4.7.

3. Results and discussion

3.1. *Potentiometry*

Previously [18] complexation between histidine and aluminum using low total aluminium concentrations (0.5–1.0 mmol dm^{-3}) and relatively high ligand to metal ratios (L : M = 5 : 1, 3 : 1) was studied. Under these conditions dominant mononuclear complexes are Al(HHis) and $Al(HHis)His^{2+}$. Only in titrations with total aluminium 0.5 mmol dm^{-3} and L : M > 3 : 1 was $Al(His)^{2+}$ detected. Dayde *et al.* [7], however, characterized interactions of histidine and aluminium with the sole complex $Al_2HisH^{3+}_{-2}$. To examine possible formation of mixed polynuclear complexes, in the present work higher total concentrations of aluminium over a wide range of histidine to aluminium ratios were used, titrating Al solutions initially at low pH with neutralized histidine solutions. These conditions should favour polymerization.

Experimentally obtained potentiometric titration data are given in figure 1. For speciation calculations data from pH 3.0 to 6.20 were selected. Fitting took account

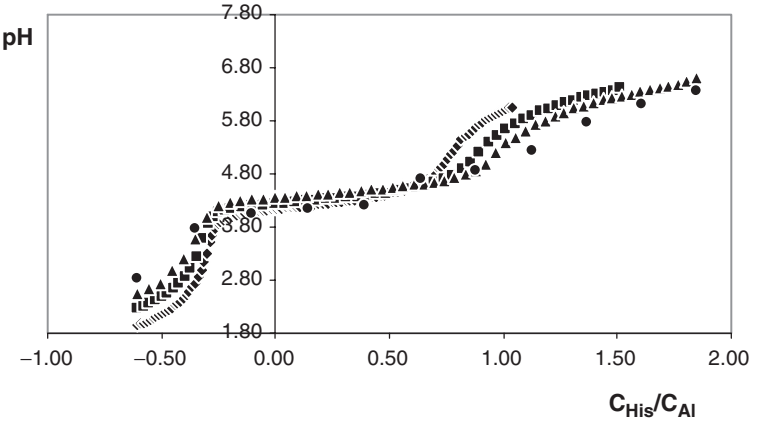

Figure 1. Titration data plotted as curves of pH *versus* concentration ratio of ligand to metal; $C_{Al} = 20$ (◆), 10 (■), 5 (▲) and 1 (●)mmol dm^{-3}. Negative values of ligand (His^-) to metal ratios denote an excess of strong acid in the titrated solution.

of the complexes AlL, AlL_2, $AlLH_{-1}$, AlL_2H_{-1}, AlLH, $AlLH_2$, AlL(LH), $Al(LH)_2$, Al_2LH, Al_2LH_{-1}, $Al_2L_2H_{-2}$ and $Al_2L_2H_{-1}$. In the first step a manual fitting option of Hyperquad was used and titration curves were processed separately. This analysis proved that at higher aluminium concentrations (20 and 10 mmol dm^{-3}) the most important species is the mixed dimer $Al_2HisH_{-1}^{4+}$. With decreasing concentrations of aluminium and increasing concentration ratios of histidine to aluminium, mononuclear complexes become increasingly important. The best fit was achieved with the complexes $Al(HHis)^{3+}$, $Al(His)^{2+}$ and $Al(HHis)His^{2+}$. When the dimer is dominant, introduction of mononuclear complexes shows that they are only minor species. However, at lower aluminium concentrations (1 to 5 mmol dm^{-3}) an acceptable fit can only be obtained by introducing these species in the model. The probable complexes and their trial stability constants were subjected to further Hyperquad refinement. In Hyperquad calculations the identity and stability of complexes which give the best fit to the experimental data are determined by minimizing the error-squares sum of the potentials, U,

$$U = \sum w_i (E_{\text{obs}} - E_{\text{calc}})^2$$

where w_i represents a statistical weight assigned to each point of the titration curve and E_{obs} and E_{calc} refer to the measured and the calculated potentials of the cell, respectively. The best model was chosen using several criteria: the lowest value of U; standard deviation in calculated stability constants less than 0.15 log units; standard deviations in potential residuals, defined as

$$s = \{ewe^T/(N-k)\}$$

where e is a vector in potential residuals ($E_{\text{obs}} - E_{\text{calc}}$), w is a weighting matrix, N is the number of observations and k is the number of refinable parameters (with standard deviation in volume readings 0.0005 cm^3 and standard deviation in potential readings 0.1 mV, s should be less than 3.0; goodness-of-fit statistics, χ^2 at the 95% confidence level with six degree of freedom less than 12.6; reasonably random scatter of potential residuals without any significant systematic trends. The refinement operations for each total aluminum concentration resulted in different and often acceptable models. Different strategies were employed in the refinement operations: fixing selected constants to simplify optimization procedure; reducing the number of experimental points included in calculations; parallel refinement of selected pure hydrolytic species together with the Al-His complexes; ''piecewise'' fitting of experimental data. Analytical parameters were always kept constant. At a total aluminum concentration of 20 mmol dm^{-3} the only accepted complex was the dimer, $Al_2HisH_{-1}^{4+}$, with rather poor statistics. Introduction of other complexes did not improve the fit. At a total aluminum concentration of 10 mmol dm^{-3} optimization commenced with this complex by fixing its stability constant and adding and refining stability constants of $Al(HHis)^{3+}$ and $Al(His)^{2+}$. The optimization ended with the acceptance of $Al(HHis)^{3+}$ and rejection of $Al(His)^{2+}$ with reasonable statistics. The two stability constants were then allowed to float and as a result the complexes $Al(HHis)^{3+}$ and $Al_2HisH_{-1}^{4+}$ were accepted (pH interval 3.5 to 5.5) with good residual trends. At total aluminium concentrations of 5 and 1 mmol dm^{-3} it was very difficult to

obtain an acceptable fit over the whole titration range. To the above model we found it necessary to add other complexes from the initial list and satisfactory results were obtained with $Al(HHis)His^{2+}$ complex, although in some models addition of $Al(His)^{2+}$ produced acceptable fits. The complexes $Al(His)_2$ and $Al(HHis)_2$ were always rejected in combination with $Al(HHis)His^{2+}$. Thus in the first optimization step a model consisting of $Al(HHis)^{3+}$, $Al(His)^{2+}$, $Al(HHis)His^{2+}$ and $Al_2HisH_{-1}^{4+}$ was established.

Previous potentiometric data [18] on Al^{3+}-histidine complexation in the pH interval 3.2–6.0 has been recalculated. Present titration data were added and in the fitting procedure the previously found model consisting of (1, 1, 1), (1, 2, 1) and (1, 1, 0) complexes was fixed. The stability constant of the (2, 1, −1) complex was varied. The optimization procedure converged and gave $\log \beta_{2,1,-1} = 6.21 \pm 0.1$. This value was then fixed and stability constants for the accepted set optimized with final values of stability constants varying slightly from those previously reported [18]; the final model involved the species (1, 1, 1), (1, 1, 0), (1, 2, 1) and (2, 1, −1). When this model was used to simulate speciation at higher aluminium concentrations, concentrations of mononuclear species were too low to be reliably detected and only complex (2, 1, −1) was sufficient to explain the experimental data. At lower aluminium concentrations, simulations showed the importance of mononuclear complexes. With this as the best model, its sensitivity was examined by co-varying the stability constant of the Al_{13}-mer with those of the accepted set, introducing the latter into the optimization procedure one by one. In the combination Al_{13}-mer + $Al(HHis)His^{2+}$, both stability constants changed. The constant of Al_{13}-mer changed from an initial value of −106.50 to −107.23, while that of the (1, 2, 1) complex changed from 20.3 to 20.1. The combination Al_{13}-mer + Al(HHis) gave for Al_{13}-mer −106.20 and 11.98 ± 0.06 for the (1, 1, 1) complex. Finally, the combination Al_{13}-mer + (2, 1, −1) gave −106.1 for the tridecamer and 6.12 ± 0.08 for the (2, 1, −1) complex. This proves that calculated stability constants of complexes are sensitive to the choice of stability constant for Al_{13}-mer. Therefore, values of stability constants of aluminum–histidine complexes with the best statistical values were fixed and values of Al_{13}-mer were varied. The obtained value ($\log \beta_{13,-32} = -106.2 \pm 0.12$) was in good agreement with that from the initial set. In the final calculation cycle all data points in the pH range 3 to 6 were used, fixing the value of the stability constant of Al_{13}-mer and refined constants of the dimer and Al(HHis)His. Calculations produced an acceptable fit (given in table 1), but some

Table 1. Calculated stability constants for the complexes in 0.1 mol dm^{-3} LiCl at 298 K. Data for protonation constants of histidine are from ref. [18].

Species	$\log \beta_{p,q,r} \pm \sigma$
H_3His^{2+}	17.01
H_2His^{+}	15.29
HHis	9.17
$Al_{13}(OH)_{32}^{7+}$	-106.20 ± 0.12
$Al(HHis)(His)^{2+}$	20.1 ± 0.08
$Al(HHis)^{3+}$	12.15 ± 0.10
$Al(His)^{2+}$	7.21 ± 0.08
$Al_2(OH)His^{4+}$	6.15 ± 0.09
Statistical parameters of the fit: $s = 3.2$–8.0, $\chi^2 = 11.9$–28.3	

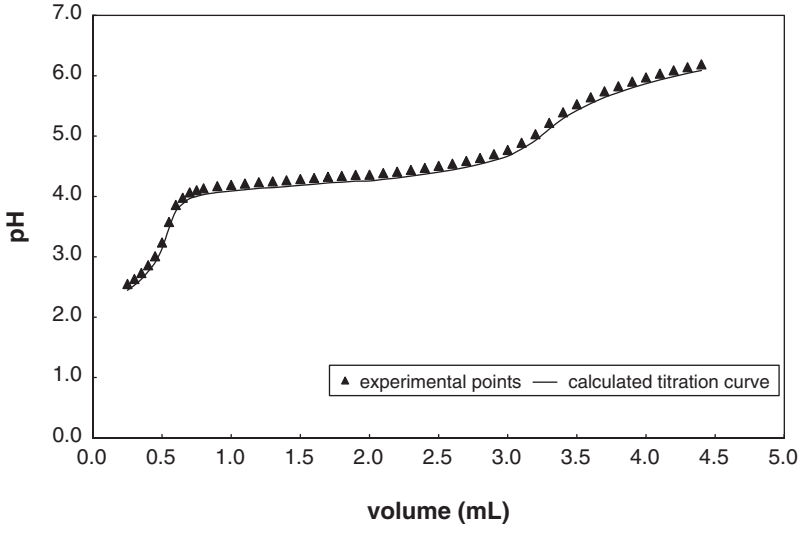

Figure 2. Experimental and calculated titration curves for a total Al^{3+} concentration of 10.0 mol dm^{-3} ($T = 298$ K, $\mu = 0.1$ mol dm^{-3}).

revision of the values determined previously [18] was needed. The complex $Al_2LH_{-2}^{3+}$ [7] was not found under the experimental conditions in this study (it may be included in the model but its inclusion worsens the statistical parameters of the fit). The diversity of species found in this work is greater than that reported by Dayde *et al*. [7], though the models in this work agree at higher aluminium concentrations and lower histidine to aluminium ratios. It should be noted that Dayde *et al*. included in their initial model the $(1, 1, 0)$ and $(1, 1, -1)$ complexes, but these were subsequently rejected on the basis of statistical parameters. Differences between the two models may be attributed to different experimental conditions. Dayde *et al*. worked at a considerably higher temperature (37°C), which significantly accelerates hydrolysis and favours polymerization. Further, the titration protocol they used, with relatively rapid measurement of potential (at 2 min intervals) may leave slowly formed aluminium–histidine complexes undetected.

3.2. *Reliability of the speciation model*

To examine the reliability of the data of table 1, the experimental (points) and calculated (lines) titration curves for a total Al concentration of 10.0 mmol dm^{-3} is plotted in figure 2. This shows that the difference between calculated and experimental data is relatively small (< 0.05 pH units). Stability constants of complexes formed in Al/His solutions are considerably higher than those reported for other aluminum-amino acid systems (table 2). The enhanced stability of the $Al(HHis)^{3+}$ complex may be explained by the formation of five-membered chelate where histidine acts as a bidentate. Maximum formation of $Al(HHis)^{3+}$ occurs around pH $\sim$ 4, which is close to the protonation constant of the imidazole group of histidine and this should facilitate proton transfer from the amine group. Another possibility concerns interaction between the aluminium ion and the π-electrons of imidazole. Such an interaction has

Table 2. Selected literature data on aluminium complexation with amino acids.

	$\log\beta \pm \sigma$					
Species	Gly	Ser	Thr	His	Asp	Glu
MLH_2					14.48 ± 0.04[b]	14.74 ± 0.04[b]
						15.03 ± 0.03[c]
MLH		11.2 ± 0.1[f]		12.21 ± 0.08[d]	11.76 ± 0.06[a]	10.88 ± 0.22[a]
					11.24 ± 0.03[b]	11.07 ± 0.06[b]
						10.68 ± 0.02[e]
						12.02 ± 0.04[f]
ML	5.91 ± 0.1[a]	5.66 ± 0.11[a]	5.51 ± 0.12[a]	7.08 ± 0.20[b]	7.87 ± 0.04[a]	7.29 ± 0.04[a]
	6.23 ± 0.1[b]	5.97 ± 0.05[b]	5.71 ± 0.08[b]	7.25 ± 0.08[d]	7.77 ± 0.02[b]	7.69 ± 0.03[b]
		5.71 ± 0.02[f]				7.86 ± 0.01[e]
						7.42 ± 0.03[f]
MLH_{-1}			0.94 ± 0.15[a]		3.30 ± 0.03	2.56 ± 0.03[f]
M_2LH_{-1}	4.35 ± 0.09[a]	3.75 ± 0.11[a]				6.68 ± 0.01[c]
		4.65 ± 0.03[f]				
M_2LH_{-2}	0.36 ± 0.04[g]	0.20 ± 0.02[g]	-0.18 ± 0.05[g]			
$K(M + HL \rightarrow MLH)$					2.14[a]	1.38[a]
						1.88[b]
						1.72[e]
						2.54[f]

[a]Ref. [11], $\mu = 0.2\,mol\,dm^{-3}$ KCl, 25°C.
[b]Ref. [25], $\mu = 0.15\,mol\,dm^{-3}$ NaCl, 37°C.
[c]Ref. [9], $\mu = 0.15\,mol\,dm^{-3}$, 37°C.
[d]Ref. [18], $\mu = 0.1\,mol\,dm^{-3}$ LiCl, 25°C.
[e]Ref. [10], $\mu = 0.1\,mol\,dm^{-3}$ KCl, 25°C.
[f]Ref. [26], $\mu = 0.1\,mol\,dm^{-3}$ LiCl, 25°C.
[g]Ref. [7], $\mu = 0.15\,mol\,dm^{-3}$ NaCl, 37°C.

been found in many transition metal complexes containing ligands with π-electron donors [24]. Since histidine is a flexible molecule it is possible that the imidazole residue not coordinated to aluminum adopts a position close to the aluminum ion due to the relatively free rotation about the CH_2 group.

The distribution diagram (figure 3) shows that $Al(HHis)^{3+}$ starts to form at pH about 2.5 and reaches maximum concentration at pH about 4.0. From this pH value the mixed binary complex $Al(HHis)(His)^{2+}$ is formed and its concentration increases with pH increase, reaching a maximum at pH around 6.0. $Al(OH)_3(aq)$ increases in concentration at pH values higher than 6.0. Formation of the tridecamer starts at pH around 4.5 and falls at pH 5.5, where the complex $Al(HHis)His^{2+}$ reaches appreciable concentration. The mixed dimer starts to form at about pH 3.5 and reaches maximum concentration at pH $\sim$ 4.2. It is the main complex at pH values $\leq$4.5. With increasing concentration of aluminium, its relative concentration increases while that of Al(HHis) rapidly decreases. Al(His) is at the limit of potentiometric detection and, bearing in mind the high concentration of $Al(OH)^{2+}$ in its region of formation, its probable composition is $Al(OH)HHis^{2+}$. The speciation diagram shows that histidine-aluminium complexes in potentiometrically accessible concentration ranges always represent a relatively small fraction of total aluminium.

3.3. *ESI-MS measurements*

Mass spectra of the histidine ($1.0\,mmol\,dm^{-3}$, pH 4.0) and aluminium chloride (1.0 and $5.0\,mmol\,dm^{-3}$, pH 3.0 and 4.0) alone were recorded under exactly the same

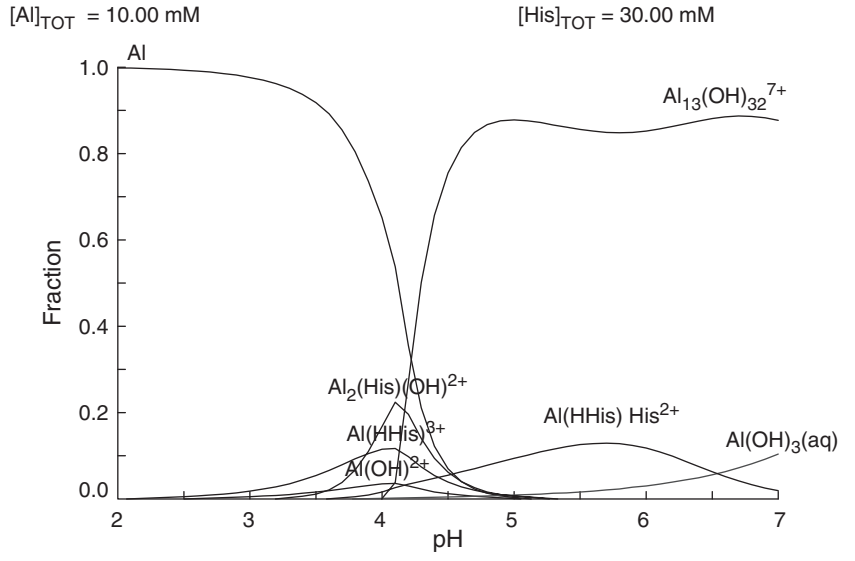

Figure 3. Distribution of histidine-Al^{3+} and hydrolysed complexes in terms of pH. The distribution was calculated with $\log \beta_{13,-32} = -106.20$ using the program Medusa [27].

experimental conditions in order to identify corresponding peaks in spectra obtained from solutions containing complexes. ESI-mass spectra gave a multitude of signals corresponding to aggregates including histidine, aluminum, sodium, chloride and hydroxide ions. It should be noted that histidine shows a strong tendency to polymerize and formation of $[(HHis)_n + H]^+$, $n = 1$–4, is evident in the spectra. Signals corresponding to histidine fragments are found at m/z 156.3 (base ion), 110, 93, 83 and 66, in agreement with the findings of El Aribi *et al.* [28]. Charge and isotopic analysis of hydrolysed aluminium solutions indicate the existence of the species, $Al_2(OH)_5^+ \cdot 2H_2O$, $Al_7O_6Cl_3(H_2O)_n^+$, $Al_{13}(OH)_{32}(H_2O)_{12}^{7+}$, $Al_3(OH)_4Cl_4 \cdot 6H_2O$ and $Al_3O_4(NaCl)_2 \cdot H_2O$. It was difficult to assign signals with m/z greater than 360 since these represent polymeric species with variable chloride and sodium ions as well as water molecules. At m/z 168 the mononuclear chloro complex $[AlCl_4^- + H^+]^0$ was identified, in accordance with the results of Sarpola *et al.* [29], but the diversity of hydrolytic species found here is much less Histidine + Al^{3+} solutions give signals not seen with histidine or aluminum chloride alone. In these solutions signal at m/z 46.2 can be assigned to $[Al_2HisH_{-1}^{4+} + Na^+]^{5+}$ while that at 117.3 can be assigned to $[Al(HHis)Cl^{2+}$, $NaCl,4H_2O + H^+]^{3+}$. Charge analysis showed that the weak signal at m/z 463 can be assigned to $[Al(HHis)HisCl_2 + H^+] \cdot 3H_2O$. These results are in agreement with the potentiometric data and thus confirm the formation of a mixed dimer in solution. Bearing in mind the concentrations of sodium and chloride ions in solutions their recombination is not unexpected, nor is the presence of coordinated chloride in Al-His complexes. Similar results have been found for oxalate-Al^{3+} solutions [30].

3.4. *^{27}Al NMR spectroscopy*

Spectra without addition of histidine were recorded using solutions in which the concentration of aluminum was 50.0 mmol dm^{-3} in the pH interval from 1.80 to

5.50, 72 h after preparation. In acidic solutions (pH < 3.0) only the peak at $\delta \sim 0$ ppm was observed. At pH values between 3.50 and 4.0 the line at $\delta \sim 0$ ppm broadened, with the appearance of a weak resonance at $\delta \sim 0.8$ ppm, weak broad resonance at 4.08 ppm and a sharp resonance at $\delta \sim 63$ ppm. The resonance at chemical shift of $\delta \sim 0$ ppm is assigned to $Al(H_2O)_6^{3+}$, broadening being due to the formation of $Al(OH)(H_2O)_2^{2+}$, while the resonances at 0.8 ppm and 4.3 ppm belong to oligomers, most probably the dimer, $Al_2(OH)_2^{4+}$ or $Al_2(OH)_4^{2+}$ and the trimer, $Al_3(OH)_4^{5+}$, respectively [31–33]. The resonance at 63 ppm is due to tetrahedral aluminium of the Al_{13}-mer "core". Increasing pH leads to the appearance of a rather broad peak at $\delta \sim 4.3$ ppm and a decrease of the intensity of the peak at 0 ppm. At the same time the solution becomes visibly turbid. At pH values higher than 5.5 (when a precipitate appeared) the peak at 4.3 ppm merges into the baseline and the resonance at $\delta \sim 0$ ppm disappears. These features are consistent with the ultimate formation of $Al(OH)_3$, which gives no signal [34]. To evaluate complexation between histidine and Al^{3+}, several series of solutions were prepared. The total concentration of histidine was 250.0, 50.0 and 25.0 mmol dm^{-3} while that of aluminium was 50.0, 12.5 and 5.0 mmol dm^{-3}. The concentration ratio of histidine to aluminium thus covered was from 3 : 1 to 10 : 1. The pH of all solutions was adjusted by addition of standard HCl or NaOH solution and solutions were left to stand for 72 h before measurements were made. A final check of pH was made 30 min before recording the spectrum. At pH 4.5 solutions became slightly turbid, but upon increasing pH up to 6.1 initial opacity disappeared. At pH 4.06, the peak at 4.3 ppm (oligomers, above) shifts to 4.69 ppm and at the same time a new broad peak at $\delta \sim 9.54$ ppm appears. The resonance at 9.54 ppm is near the expected value of $\delta \sim 10$ ppm when an amino acid acts as a bidentate [35]. In this pH region the dominant complexes are $Al(HHis)^{3+}$ and the dimer, $Al_2HisH_{-1}^{4+}$. Therefore, the resonance at 9.54 ppm is attributed to $Al(HHis)^{3+}$ and that at 4.69 ppm to the dimer. Bearing in mind that pK value of the imidazole nitrogen is about 6.5, it appears that the proton resides on this site. Thus it may be assumed that $Al(HHis)^{3+}$ is formed by binding the carboxylate oxygen and amino groups to aluminium. Considering the equilibrium

$$Al(H_2O)_6^{3+} + H_2His^+ \leftrightarrow Al(H_2O)_4(HHis)^{3+} + H^+ + 2H_2O,$$

for which the equilibrium constant is given by the expression $\log K_{eq} = \log \beta_{1,1,1} - \log \beta_{0,2,1} = -3.14$, it is seen that it is less probable than the equilibrium

$$Al(H_2O)_6^{3+} + HHis \leftrightarrow Al(H_2O)_4(HHis)^{3+} + 2H_2O,$$

for which the equilibrium constant is $\log K_{eq} = \log \beta_{1,1,1} - \log \beta_{0,1,1} = 2.98$, in line with those of other bidentate amino acids. Since the above reaction is dynamic, broadening of resonances at 0 and 9.54 ppm is observed. HHis represents the protonated histidine molecule in which the proton from the ammonium group, in the presence of aluminium, is transferred to the imidazole residue. Further increase of pH to 4.55–5.54, leads to shifting and merging of the band at 4.3 ppm into the tail of the resonance at ~8.44 ppm with the appearance of a new resonance at ~12.08 ppm. The resonance at 8.44 ppm represents the upfield shift of the resonance at 9.54 ppm, while the resonance at 12.08 ppm indicates the formation of a new complex. Increasing pH to 6.04 causes both resonances to shift upfield to 8.2 and 11.96 ppm,

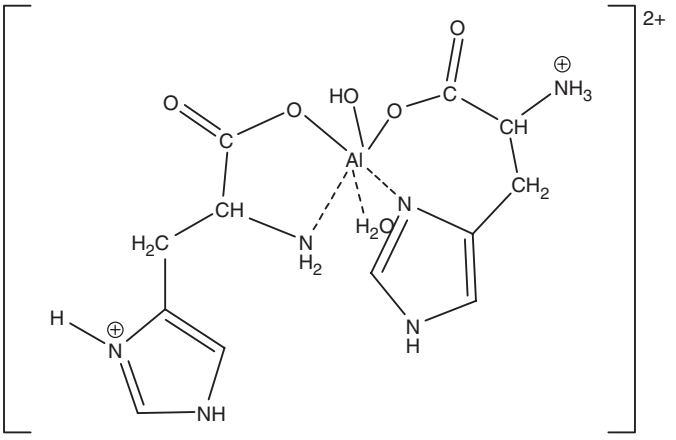

Scheme 1. Tentative structure of aluminium–histidine complex.

respectively. At the same time the intensity of the sharp resonance at 63 ppm decreases. The resonance at ~12 ppm may be attributed to mixed binary complex Al(HHis)His^{2+}.

The structure of this complex may involve coordination of one histidine molecule via the formation of a five-membered ring and the other histidine molecule in a seven-membered ring as shown diagramatically in scheme 1. The fifth coordination site is occupied by a hydroxyl group and a water molecule is bound to the sixth. The side chain is as flexible as in aspartic or glutamic acid and the formation of the seven-membered ring is sterically feasible. The coordination sphere around aluminium is distorted octahedral so that the aluminium resonance is shifted further downfield in comparison with that originating from more symmetric five- and six-membered ring, as with aspartic acid ($\delta \sim 10$ ppm).

3.5. *^{13}C NMR spectra*

Proton-decoupled ^{13}C NMR spectra were measured for solutions in which the total concentration of histidine was 0.1 mol dm^{-3} and that of aluminium 0.1 or 0.2 mol dm^{-3} at pH 3.20. Assignment of carbon atoms is given in scheme 2. The spectrum of free histidine (0.1 mol dm^{-3}, pH 3.21, 25°C) shows six resonances at 31, 58.5, 123, 133, 139.5 and 177 ppm, arising from aliphatic β-CH_2, α-CH, imidazole 5-CH, 4-CH, 2-CH and carboxylic C-atoms, respectively. New signals appear upon addition of aluminium to histidine solutions and are indicative of the presence of histidine bound to aluminium. These new resonances appear upfield of free histidine signals. For aliphatic CH_2 and CH carbons the chemical shift differences between free and bound histidine were 0.4 ppm, imidazole 4-C, 0.3 ppm, and carboxylic carbon 0.8 ppm. The intensity of free histidine carboxylic resonance is considerably lowered upon addition of aluminium and further decreases on increasing the aluminium concentration. Separation of free and bound signals indicates relatively slow exchange between the coordination sphere and the bulk solution. The main resonances from aliphatic C atoms in free histidine show slight upfield shifts upon addition of aluminium. This result could be explained by the involvement of both carboxyl and amino groups in coordination. The speciation diagram indicates that under the conditions of ^{13}C NMR spectrum the dominant complex in the solution is $Al(HHis)^{3+}$ together

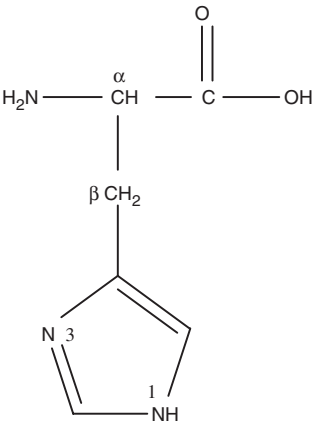

Scheme 2. Assignment of carbon atoms in histidine.

with small amounts of hydrolysed oligomers. Hence, in ^{13}C NMR spectra of $Al(HHis)^{3+}$, changes in position of resonances seen down the whole aliphatic carbon chain are consistent with the closure of the five-membered ring.

3.6. *The [Al(OH)(HHis)$_2$]Cl$_2$ complex*

Elemental analyses agree with the formula $[Al(OH)(HHis)_2]Cl_2$ or $[Al(HHis)His]Cl_2$. Differential scanning calorimetry (DSC) analysis shows that the compound decomposes upon heating in five steps. For comparison histidine melts at 279–284°C. The mass loss corresponding to these processes were 4.48, 5.40, 8.90, 13.32 and 9.83 wt%, respectively. Total mass loss was 40.8%. A first broad peak at 46°C corresponds to water loss and the second at 146.9°C to loss of HCl. Between 234 and 282°C, melting and decomposition of histidine commences, in line with observations of other transition metal-histidine complexes [36]. From 282 to 400°C decomposition of histidine and formation of aluminium-oxide is completed. IR spectra of the complex show changes in position and shape of some bands as compared to those of free *S*-histidine (table 3). The data can be interpreted on the basis of literature data for similar metal-histidine complexes [37–40]. In the range 1629–1567 cm^{-1} are observed the asymmetric carboxylate stretch and amino group bending. In the range 1498–1284 cm^{-1} is observed the symmetric COO^- stretch and the symmetric NH_2 bending vibrations and in the range 1121–500 cm^{-1} is observed wagging COO^-, twisting NH_3^+, and imidazole ring vibrations. A broad band situated at 3100–2800 cm^{-1} in free histidine disappears and splits into several smaller sharp bands in the spectrum of the complex. This indicate disruption of CO—NH hydrogen bond [41] due to coordination of carboxylate to aluminium. The carboxylate stretching band at 1412 cm^{-1} (νCOO^-) shifts to lower frequency and its intensity decreases while $\nu_{as}COO^-$ and νC=C(ring) at 1584 and 1567 cm^{-1}, respectively, produce a single band at 1577 cm^{-1}. The νC=N band of the imidazole ring is observed at 1512 cm^{-1} and in the complex is shifted to 1498 cm^{-1} with decrease in intensity. These observations indicate the participation of carboxylate, amino and heterocyclic nitrogen in coordination.

Table 3. IR data for histidine and the isolated aluminium complex (cm^{-1}).

Complex	Histidine	Assignment
3407		ν_sN–H
		ν_{as}N–H
	3138	
3108		
3045	3018	
2923		
2856	2873	
2098	2022	δ_{as}N–H
2007		
1629	1635	δ_{as}N–H + $\nu_{as}COO^-$
1604		$\nu_{as}COO^- + \nu_{ring}C{=}C$
1577	1584, 1567	
1498	1512, 1494	$\nu_{ring}C{=}N + \delta NH_3^+$
1459	1454	
1427		
1410(m)	1412(b)	$\nu_s COO^-$
1381		
1333	1342	ϖCH_2
1308	1312	$\delta_{ring}CH$
1284		
1121	1110	$\nu_{as}CCN$
979	978	ρCH_2
866	852	$\delta_{ring} + \delta_c CCN$
683(w)	682(s)	γ_{ring}C–H, ϖCOO^-
646	653	δC–H(ring)
624(b,m)	628(vs)	δCOO^-
538	537	ρCOO^-

4. Conclusions

Histidine and aluminium ion form dinuclear and mononuclear binary and mixed complexes in which histidine is bound to aluminium in bidentate fashion to form five- and possibly seven-membered chelate rings. The latter can occur at pH values where deprotonation of imidazolium is appreciable (pH > 5). Complexation is accompanied by pronounced hydrolysis of aluminum ion. Stability constants for complex formation indicate that histidine behaves like other bidentate amino acids but binds far less strongly than other gi and serum carboxylic acids [42].

Acknowledgements

The authors would like to thank Dr Istvan Banyai (Debrecen, Hungary) for help with NMR measurements. The financial help from the Serbian Ministry of Science and Technology under project 1941 is gratefully acknowledged.

References

[1] Special recent issues of journals devoted to aluminum toxicity and chemistry are: *J. Inorg. Biochem.*, **97**(1) (2003); **87**(1–2) (2001); **76**(2) (1992); *Coord. Chem. Rev.*, **228**(2) (2002); **149** (1996).
[2] P. Nayak. *Environ. Res. A*, **89**, 101 (2002).
[3] J.H. Gitelman (Ed.). *Aluminum and Health. A Critical Review*, Marcel Dekker, New York (1989); G.F. van Landeghem, M.E. de Broe, P.C. D'Haese. *Clinical Biochem.*, **31**, 385 (1998).

[4] A. Martell, R.D. Hancock, R.M. Smith, R.J. Motekaitis. *Coord. Chem. Rev.*, **149**, 311 (1996); A.E. Martell, R.J. Motekaitis, R.M. Smith. *Polyhedron*, **9**, 171 (1990).
[5] R.J.P. Williams. *Coord. Chem. Rev.*, **149**, 1 (1966); A.C. Alfrey. In *Handbook of Metal-Ligand Interactions in Biological Fluids, Vol. 2. Bioinorganic Medicine*, G. Berthon (Ed.), pp. 735–740, Marcel Dekker, New York (1995).
[6] T. Kiss, T. Jakusch, M. Kilyen, E. Kiss, A. Lakatos. *Polyhedron*, **19**, 2389 (2000); C. Orvig. In *Coordination Chemistry of Aluminum*, G.H. Robinson (Ed.), pp. 85–121, VCH, Weinheim (1993).
[7] S. Dayde, D. Champmartin, P. Rubini, G. Berthon. *Inorg. Chim. Acta*, **339**, 513 (2002).
[8] E. Kiss, A. Lakatos, I. Banyai, T. Kiss. *J. Inorg. Biochem.*, **69**, 145 (1998).
[9] S. Dayde, V. Brumas, D. Champmartin, P. Rubini, G. Berthon. *J. Inorg. Biochem.*, **97**, 104 (2003).
[10] X. Yang, Y. Tang, S. Bi, G. Yang, J. Hu. *Anal. Sci.*, **19**, 133 (2003).
[11] T. Kiss, I. Sovago, I. Toth, A. Lakatos, P. Bertani, A. Tapparo, G. Bombi, R.B. Martin. *J. Chem. Soc., Dalton Trans.*, 1967 (1997).
[12] S. Laurie. In *Comprehensive Coordination Chemistry*, Vol. 2, G. Wilkinson, R.D. Gillard and J.A. McCleverty (Eds), pp. 739–776, Pergamon Press, Oxford (1987); H.D. Jakubke, H. Jeshkeit. *Aminosauren, Peptide, Proteine*, Akademie Verlag, Berlin (1982).
[13] G.B. van der Voet. In *Aluminum in Biology and Medicine*, pp. 109–122, Ciba Foundation Symposium 169, Wiley, Chichester (1992).
[14] *The Merck Manual of Diagnosis and Therapy*, 17th edition, Merck & Co., New Jersey (2003); H. Levy. *Histidinemia*, Orphanet Encyclopedia, 2002. Available online at: http://www.infobiogen.fr/patho/GB/uk-HIS.html; *Public Health Goal for Aluminum in Drinking Water*, Office of Environmental Health Hazard Assessment, California Environmental Protection Agency, California (2001); *Aluminum Compounds, Review of Toxicological Literature*, Integrated Laboratory Systems, National Institute of Environmental Health Sciences, Research Triangle Park, North Carolina (2000).
[15] P. Zatta, A. Taylor, P. Zambenedetti, R. Milacic, P. Dell'Antone. *Life Sci.*, **66**, 2261 (1999).
[16] K. Atkari, T. Kiss, R. Bertani, R.B. Martin. *Inorg. Chem.*, **35**, 7089 (1996).
[17] P. Charlet, J.P. Deloume, G. Duc, G. Thomas-David, *Bull. Soc. Chim. Fr.*, **7–8**, 222 (1984).
[18] P. Djurdjevic, R. Jelic, D. Dzajevic, M. Cvijovic. *Metal Based Drugs*, **8**, 235 (2002).
[19] F.J.C. Rossotti, H. Rossotti. *The Determination of Stability Constants*, pp. 58–62, McGraw Hill Inc., New York (1961).
[20] P. Gans, A. Sabatini, A. Vacca. *Talanta*, **43**, 1739 (1996).
[21] P. Gans, A. Sabatini, A. Vacca. *J. Chem. Soc., Dalton Trans.*, 1195 (1985).
[22] A. Singhal, K.D. Keefer. *J. Mater. Res.*, **9**, 1973 (1994); L.O. Ohman, S. Sjoberg, N. Ingri. *Acta Chem. Scand. Ser. A*, **37**, 561 (1983); T. Hedlund, S. Sjoberg, L.O. Ohman. *Acta Chem. Scand. Ser. A*, **41**, 197 (1987).
[23] M. Marinkovic, V. Antonijevic. *Spectrochim. Acta*, **35B**, 129 (1980).
[24] G. Bogdanovic, A.S. de Bire, S. Zaric. *Eur. J. Inorg. Chem.*, 1599 (2002).
[25] S. Dayde. These de Doctorat de l'Universite Paul Sabatier, Toulouse (1990).
[26] P. Djurdjevic, R. Jelic. *Main Group Metal Chemistry*, **21**, 331 (1998).
[27] I. Puigdomenech. *Input, Sed and Predom: Computer programs drawing equilibrium diagrams*, Technical report TRITA-OOK-3010. Royal Institute of Technology, Department of Inorganic Chemistry, Stockholm (1983).
[28] H. El Aribi, G. Orlova, A.C. Hopkinson, K.W.M. Siu. *J. Phys. Chem. A*, **108**, 3844–3853 (2004).
[29] A. Sarpola, V. Hietapelto, J. Jalonen, J. Jokela, R.S. Laitinen. *J. Mass Spectrometry*, **39**, 423 (2004).
[30] T. Umemura, K. Asaka, K. Sekizawa, T. Odake, K. Tsunoda, K. Satake, Q. Wang, B. Huang. *Anal. Sci.*, **17**, 149 (2001).
[31] J.W. Akitt. *Prog. Nucl. Mag. Res. Spectr.*, **21**, 1 (1989).
[32] K.L. Perry. J. Shafran. *J. Inorg. Biochem.*, **87**, 115 (2001).
[33] L.O. Ohman, S. Sjoberg. *Coord. Chem. Rev.*, **149**, 33 (1996).
[34] J.A. Tossell. *Geochim. Cosmochim. Acta*, **65**, 2549 (2001); M.P. Bertsch, D.R. Parker. In *The Environmental Chemistry of Aluminum*, G. Sposito (Ed.), 2nd Edn, pp. 117–168, Lewis Publ., Boca Raton, FL (1996),.
[35] S.B. Karweer, B.P. Pillai, R.K. Iyer. *Magnetic Res. Chem.*, **28**, 922 (1990); S.B. Karweer, B.P. Pillai, R.K. Iyer. *Indian J. Chem.*, **30A**, 1064 (1991).
[36] S. Materazzi, R. Curini, G. D'Ascenzo. *Thermochim. Acta*, **275**, 93 (1996).
[37] S.R. de Andrade Leite, M.A. Couto dos Santos, C.R. Carubelli, A.M. Galindo Massabni. *Spectrochim. Acta A*, **55**, 1185 (1999).
[38] V. Balice, T. Theophanides. *J. Inorg. Nucl. Chem.*, **32**, 1237 (1970).
[39] A. Barth. *Prog. Biophys. Mol. Biol.*, **74**, 141 (2000).
[40] M. Cordes, J.L. Walter. *Spectrochim. Acta A*, **24**, 237 (1968).
[41] I. Bennett, A.G.H. Davidson, M. Harding, I. Morelle. *Acta Cryst.*, **B26**, 1722 (1970).
[42] P. Rubini, A. Lakatos, D. Champmartin, T. Kiss. *Coord. Chem. Rev.*, **228**, 137 (2002); S. Dayde, G. Berthon. *Food Additives and Contaminants*, **7**, S155 (1990).